Puzzolo and Mallamaci *Neural Development* 2010, **5**:8
http://www.neuraldevelopment.com/content/5/1/8

Neural Development

RESEARCH ARTICLE Open Access

Cortico-cerebral histogenesis in the opossum *Monodelphis domestica*: generation of a hexalaminar neocortex in the absence of a basal proliferative compartment

Elisa Puzzolo, Antonello Mallamaci*

Abstract

Background: The metatherian *Monodelphis domestica*, commonly known as the South-American short-tailed opossum, is an appealing animal model for developmental studies on cortico-cerebral development. Given its phylogenetic position, it can help in tracing evolutionary origins of key traits peculiar to the eutherian central nervous system. The capability of its pup to regenerate damaged cortico-spinal connections makes it an ideal substrate for regenerative studies. Recent sequencing of its genome and the *ex utero* accessibility of its developing cerebral cortex further enhance its experimental interest. However, at the moment, a comprehensive cellular and molecular characterization of its cortical development is missing.

Results: A systematic analysis of opossum cortico-cerebral development was performed, including: origin of cortical neurons; migration of these neurons from their birthplaces to their final layer destinations; and molecular differentiation of distinct neocortical laminae.
We observed that opossum projection neurons and interneurons are generated by pallial and subpallial precursors, respectively, similar to rodents. A six-layered cortex with a eutherian-like molecular profile is laid down, according to the inside-out rule. However, neocortical projection neurons are generated by apical neural precursors and almost no basal progenitors may be found in the neuronogenic neopallial primordium. In the opossum neocortex, *Tbr2*, the hallmark of eutherian basal progenitors, is transiently expressed by postmitotic progenies of apical precursors prior to the activation of more mature neuronal markers.

Conclusions: The neocortical developmental program predates Eutheria-Methatheria branching. However, in metatherians, unlike eutherians, a basal proliferative compartment is not needed for the formation of a six-layered neuronal blueprint.

Background

The marsupial South-American short-tailed opossum, *Monodelphis domestica*, is an appealing animal model for developmental studies on cortico-cerebral development for a variety of reasons. First is the phylogenetic position of marsupials, with its implications. Metatherians (or marsupials) are one of the three subclasses of modern mammals, the other two being prototherians (or monotremes) and eutherians (commonly referred to as placentals). Branching between modern sauropsides and mammals took place about 300 million years (My) ago; separations among mammalian subclasses were more recent, 180 My ago for eutherian/metatherian lineages [1], and around 210 My ago for the prototherian lineage [2,3]. Accordingly, marsupials can provide a valuable tool for tracing evolutionary origins of key traits peculiar to the placental central nervous system (CNS). A second reason for our interest is that the opossum pup is able to regenerate connections between neurons of the cerebral cortex and spinal cord damaged by experimental trauma, which makes it an ideal substrate for regenerative studies [4-7]. Third, since the opossum cortex mainly develops after birth, newborns

* Correspondence: amallama@sissa.it
International School for Advanced Studies (SISSA/ISAS), Trieste, Italy

BioMed Central

© 2010 Puzzolo and Mallamaci; licensee BioMed Central Ltd. This is an Open Access article distributed under the terms of the Creative Commons Attribution License (http://creativecommons.org/licenses/by/2.0), which permits unrestricted use, distribution, and reproduction in any medium, provided the original work is properly cited.

of this species are particularly suitable for early *ex utero* micro-surgical manipulations of such structures [8,9]. Fourth, the complete *M. domestica* genome has recently been sequenced [10], facilitating molecular studies on this model. Important also is that *Monodelphis* is particularly suitable for laboratory studies since it is small, has a short gestational period (2 weeks) and reproduces prolifically throughout the year [8].

Until recently, marsupial cortico-cerebral development has been commonly investigated using classic histology methods [11]. A hexalaminar cortical organitazion, similar to the placental one, has been recognized in *M. domestica* and *Didelphis virginiana* [8,12], and an 'inside-out' gradient of neuronal generation has been assessed in *Trichosurus vulpecula* [13]. Thalamo-cortical connectivity has also been studied by lipophylic dye tracing [14]. However, several features of *Monodelphis* corticogenesis are unknown. The generation times of distinct neocortical laminae have not been determined, knowledge of their molecular diversification is relatively poor, and little is known about where and how distinctive neocortical neuron types are generated. Glutamatergic neurons might largely originate from progenitors within the pallial ventricular zone (VZ), since a basal progenitor compartment, corresponding to the source of the vast majority of neocortical projection neurons in placentals [15-17], appears in the opossum only at late developmental stages [18,19]. Conversely, GABAergic interneurons might arise from the ventral telencephalon, as in other amniota [20-22]. However, both issues have still to be experimentally addressed.

Nowadays, the large body of molecular tools and methodologies used for developmental studies on the cortex of placentals is suitable for addressing cortical histogenesis in marsupials in detail. The availability of *M. domestica* genomic sequence data makes their exploitation even more feasible. Taking advantage of these tools, we tried to fill gaps in our knowledge of opossum corticogenesis, studying the origin of cortical neurons, their laminar differentiation and their migration profiles from periventricular layers to their final layer positions.

Results

Molecular differentiation of neurons belonging to distinct neocortical laminae and their radial migration

The placental neocortex is formed of six layers, each expressing a well defined set of molecular markers [23]. To assay possible conservation of the neocortical laminar profile between placentals and marsupials, we looked at the distribution of a selection of these markers in the opossum neocortex at postnatal day (P)30, a developmental age at which radial neuronal migration seems to be largely completed (Figure 1A). Tbr1, expressed by mouse subplate, marginal zone and layer VI (as well as, to a lesser extent, layers III and II) [24], was detectable in the opossum in two stripes of cells. The deeper, corresponding to layer VI, included stronger labeled neurons; the more superficial, corresponding to layers II and III, displayed less intense immunoreactivity. Only a few weakly labelled Tbr1^{+} cells were found in layer I, if any. Foxp2 and Tle4, markers of deep layers in placentals, were both confined to the deep grey matter of the opossum. As expected, Tle4, expressed by mouse layers VI and V, displayed a wider radial domain compared to Foxp2, restricted to murine layer VI only [24]. Conversely, Cux1 and Brn1, markers of upper layers in placentals, were both confined to the superficial grey matter. Again as expected, Brn1, also labeling a subset of layer V neurons in the mouse [25], displayed a wider radial domain compared to Cux1, a marker of layers II to IV only [26].

Next, to reconstruct the temporal order of layer generation, we followed two complementary approaches. First, we assayed the time-course of expression of selected laminar markers, Tle4, Foxp2, and Cux1 for cortical plate (CP) as well as Calretinin and *Reelin* (*Reln*) mRNA for preplate (PPL). Second, we performed systematic bromodeoxyuridine (BrdU) pulse-chase birthdating analysis.

Time-course analysis of laminar markers gave results similar to the mouse. There were, however, some differences. As for Foxp2, no neocortical signal was detectable at P0, when a few strongly labeled cells were conversely present in basal ganglia (data not shown). A Foxp2 signal appeared in lateral neocortex by P4. At P8, this signal spread to the entire cortical plate, becoming progressively confined to the deepest part of it at later developmental ages (Figure 1B). A similar profile was displayed by the deep cortical plate marker Tle4 (data not shown and Figure 1C). As for Cux1 (Figure 1D), two weak and hardly detectable signals were found at P10, in periventricular layers and in a few cells in the upper cortical plate. These signals were stronger at P12, and, by P18, the abventricular expression domain became wider than the periventricular one. By P25, Cux1^{+} cells were tightly clustered in the most superficial cortical plate and no more Cux1 was detectable near the ventricle.

Calretinin (Calb2), expressed by mouse subplate and Cajal-Retzius cells, was detectable in the opossum telencephalon throughout neuronogenesis (Figure 2A). At P1, Calretinin^{+} cells were mainly localized in the ventral telencephalon and, within the cortex, restricted to the most marginal-lateral part of it (Figure 2Aa,a', arrowheads). At P4, positive cells were throughout the cortical plexiform layer (PPL), including the hippocampus; within the lateral cortex, the Calretinin^{+} domain was split into two stripes, the more superficial including the

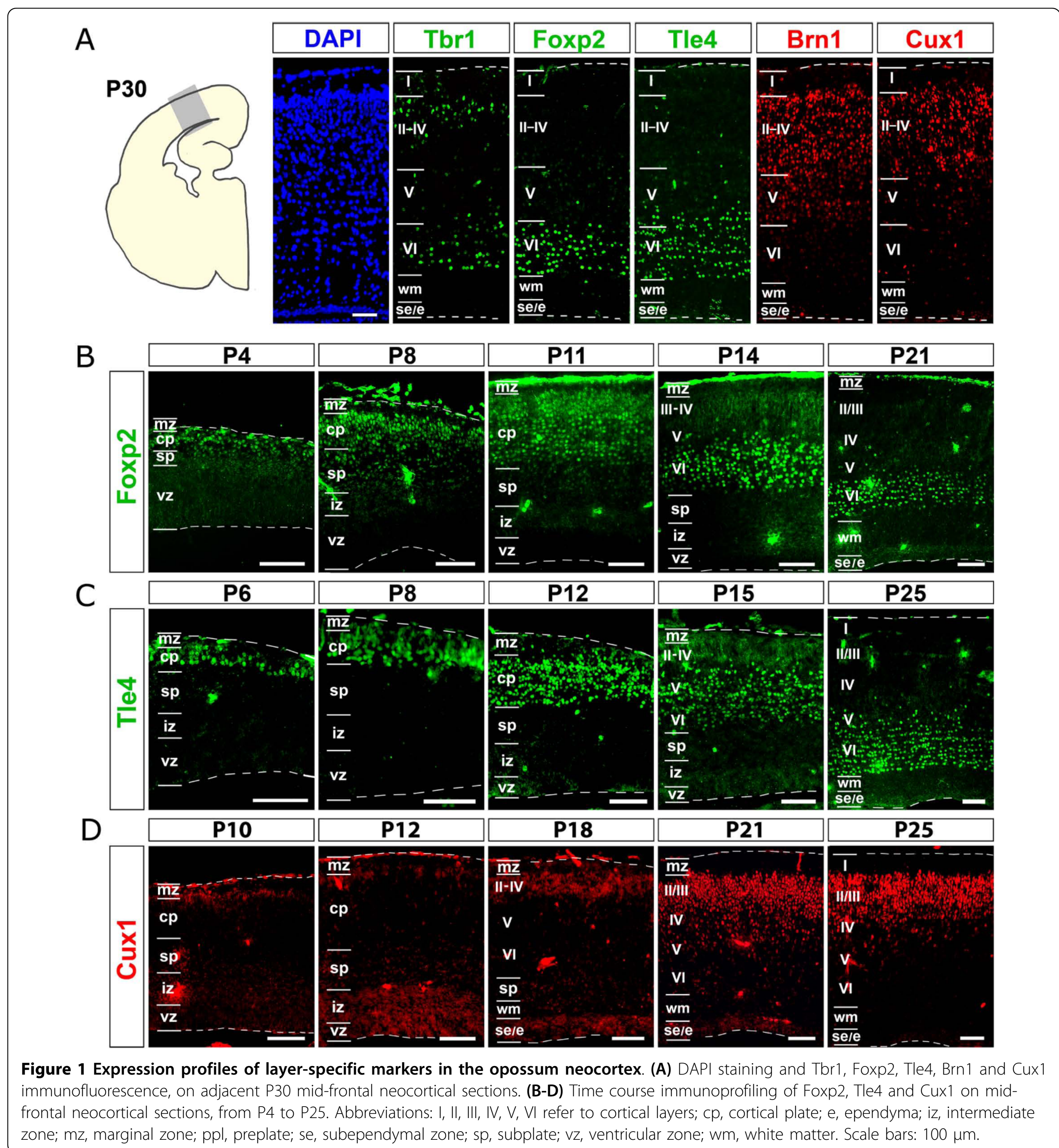

Figure 1 Expression profiles of layer-specific markers in the opossum neocortex. **(A)** DAPI staining and Tbr1, Foxp2, Tle4, Brn1 and Cux1 immunofluorescence, on adjacent P30 mid-frontal neocortical sections. **(B-D)** Time course immunoprofiling of Foxp2, Tle4 and Cux1 on mid-frontal neocortical sections, from P4 to P25. Abbreviations: I, II, III, IV, V, VI refer to cortical layers; cp, cortical plate; e, ependyma; iz, intermediate zone; mz, marginal zone; ppl, preplate; se, subependymal zone; sp, subplate; vz, ventricular zone; wm, white matter. Scale bars: 100 μm.

marginal zone (MZ), the deeper corresponding to the subplate (SP) (Figure 2Ab,b'). This SP domain, relatively wider compared to the mouse one (Figure 2Ac,c',d,d'), persisted up to P18 (Additional file 1A), disappearing around P20 (Additional file 1B, C). This domain was separated from the ventricular Pax6 domain by the interposed intermediate zone (IZ; Figure 2Ae,e') and abutted the layer VI-V Tle4 domain on its marginal side (Figure 2Af). However, Calretinin was not restricted to PPL and its derivatives. From P4 until P18, weaker labeled Calretinin$^+$ cells were detectable within the outmost cortical plate, where the last generated neurons settle (Figure 2Ab,c',d'; Additional file 1A). Starting from P20 and, better, at P30, a distinct, areally restricted, strong Calretinin expression domain was evident a few cell rows deeper to the MZ (Additional file 1B-F).

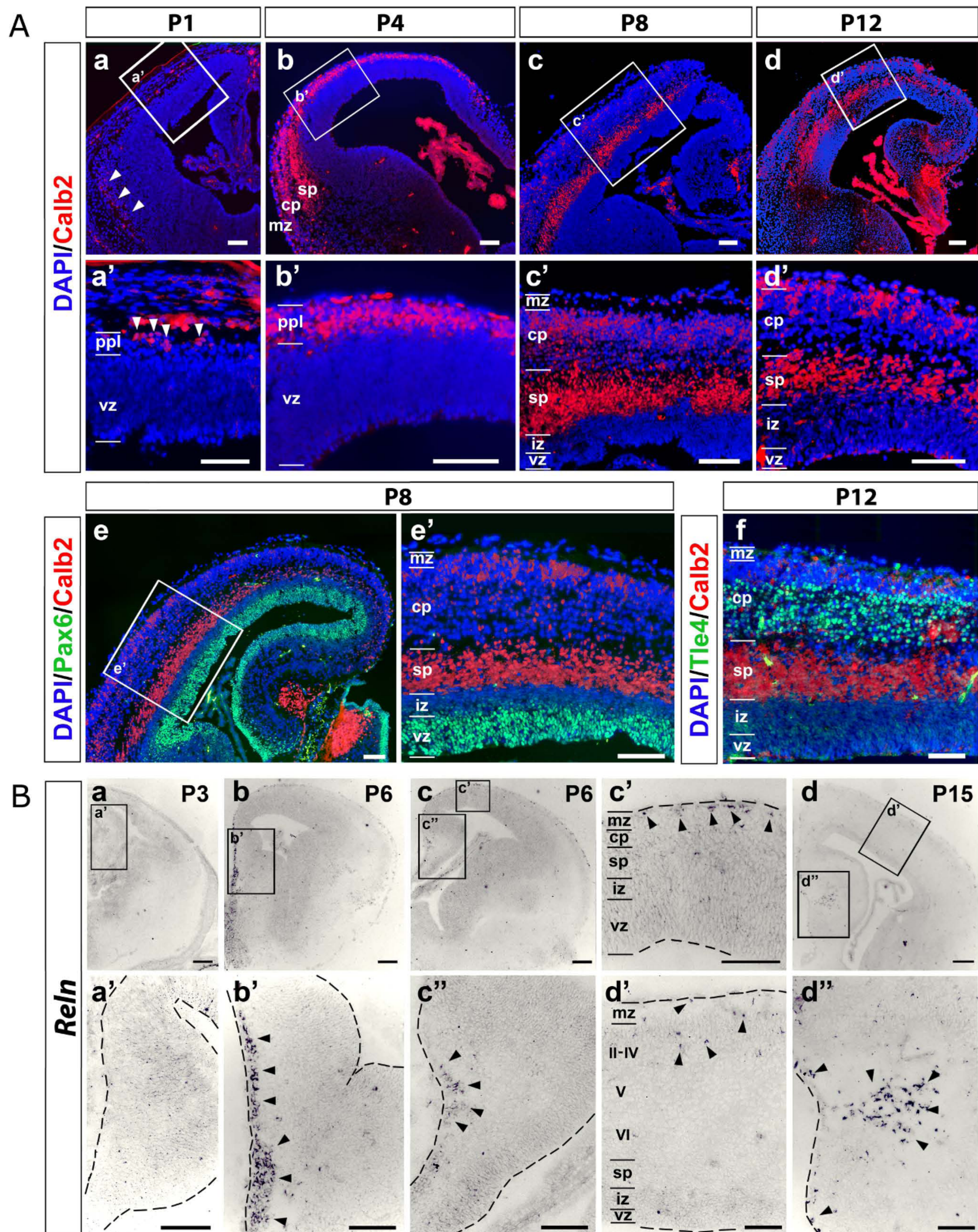

Figure 2 Dynamics of Calretinin and Reelin expression in the developing opossum telencephalon. **(Aa-d)** Time course immunoprofiling of Calretinin (Calb2) from P1 to P12. **(Aa'-d')** Magnifications of boxed areas in (Aa-d). **(Ae-f)** Comparisons among distributions of Calretinin, Pax6 (Ae,e') and Tle4 (Af). **(B)** *In situ* hybridization of *Reelin* (*Reln*) mRNA on coronal sections of P3, P6 and P15 opossum telencephalons. (Ba'-d") are magnifications of boxed areas in (Ba-d). Abbreviations: II-IV, V, VI refer to cortical layers; cp, cortical plate; iz, intermediate zone; mz, marginal zone; ppl, preplate; sp, subplate; vz, ventricular zone. Scale bars: 100 μm. Arrowheads in A point to Calb2$^+$ cells within the ppl (a,a'); arrowheads in B point to *Reln*$^+$ neurons at around the septo-pallial border (b,b'), in the neocortical marginal zone (c,c'), the cortical hem (c,c",d,d"), the neocortical outer cortical plate (d,d').

As for Reelin, this glycoprotein is a hallmark of Cajal-Retzius cells in the mouse, where additional *Reln*$^+$ cells can also be found in layers IV-V of the late cortical plate [27-29]. We studied *Reln* expression in the opossum by a riboprobe corresponding to exons 1 to 12 and found a spatio-temporal profile similar to the mouse one (Figure 2B). No *Reln* signal was detectable in the pallium at P3, that is, just before the appearance of the CP (Figure 2Ba,a'). Three days later, however, at P6, numerous *Reln*$^+$ cells were found in the neocortical MZ (Figure 2Bc,c'), as well as in the marginal cingulate cortex (Figure 2Bb,b') and in the stratum lacunosum-moleculare of the hippocampus (Figure 2Bc,c"), that is, near two of the main birthplaces of Cajal-Retzius cells described in placentals [29,30]. This expression pattern was retained at least up to P15. At this age *Reln*$^+$ cells within the neocortical MZ were much more sparse and additional *Reln*$^+$ elements were detectable within the developing neocortical CP (Figure 2Bd-d").

To reconstruct the temporal order of layer generation, we also performed systematic BrdU pulse-chase birth-dating analysis. By this approach, cells which were in S-phase at the time of BrdU injection and exited the cell cycle immediately afterwards, remained heavily labeled and, as such, easily traceable upon completion of their radial migration. We injected opossum pups at different developmental ages (P1, P4, P6, P8, P10, P12, P14, P16, and P18) with a single pulse of saturating BrdU and left them to develop until the age of P30, when all neurons have reached their final laminar position (as shown in Figures 1 and 2). We recovered their brains and analyzed the cortices by BrdU immunofluorescence (Figure 3A). To compare radial distribution and laminar identities of BrdU$^+$ cells in distinct brains, we divided the cortical wall into 20 equally spaced bins, numbered from ventricular to marginal, and on this framework reported the approximative radial extension of distinct cortical laminae: layer I (evaluated by loose DAPI staining), layers II-IV (by Cux1 immunofluorescence), and layers V-VI (by Tle4 immunofluorescence). Then, for each injection time, we counted BrdU$^+$ cells, calculated the percentage of them falling into each bin and plotted the data. Finally, we superimposed the resulting curves, obtaining a synopsis of the whole radial migration process (Figure 3B).

We found that neocortical neurons were generated in a wide temporal window, mainly from P1 to P14. Cells born at P16 reached superficial layers only to a limited extent, suggesting that at that age neurogenesis was over, and P18 cells prevalently remained beneath the CP. Deep cortical plate neurons were prevalently born between P1 and P6, and upper cortical plate neurons between P8 and P14. Colocalization of Tle4 and Cux1 with BrdU in P30 animals injected at P4 and P12, respectively, confirmed this conclusion (Figure 3C, D). As the SP is not anymore distinguishable at P30, we assayed the date of birth of its neurons in distinct, dedicated experiments. By administering P1 pups with BrdU and recovering their brains at P7 and P12, BrdU$^+$/Calretinin$^+$ cells were detectable beneath the CP, especially in lateral cortex (Figure 3E and data not shown), suggesting that the SP is mainly generated around birth. Finally, consistent with *Reln* data, P1 BrdU-pulsed/Calretinin$^+$ cells, corresponding to presumptive Cajal-Retzius cells [31], were also detectable at P7 in the neocortical MZ (Figure 3F), the marginal cingulate cortex (Figure 3G), and the hippocampal stratum lacunosum-moleculare (Figure 3H).

In conclusion: in the opossum, neocortical neuronogenesis begins at the time of birth and ends 2 weeks later, at P14 to P16, and radial migration is completed by P25; the molecular laminar profile is very similar in marsupials and placentals; and after PPL splitting, cortical plate neurons are laid down in both mammalian subclasses according to the same 'inside-out' rule.

Does a basal progenitor compartment exist in the opossum?

In placentals, neocortical projection neurons are prevalently generated by basal progenitors or intermediate progenitor cells, which lie around the pallial subventricular zone-VZ border and divide far from the ventricular surface [16,17]. In the developing opossum cortex, a subventricular zone is not morphologically distinguishable [8]. A basal proliferative compartment has been reported recently [19], although only after neuronogenesis completion (Figure 3B). We systematically readdressed this issue by assaying mitosis distribution and immunoprofiling distinct neuronogenic progenitors throughout the neuronogenetic window and beyond.

First, we studied the distribution of cortical progenitors undergoing mitosis at distinct radial positions, starting from P1 up to P25, by scoring the mitotic marker phospo-histone 3 (pH3) (Figure 4A). For each developmental age, we divided the cortical wall into four unequally spaced bins, *l* (luminal, including the two ventricular most cell rows), *p* (periventricular, corresponding to the densely packed zone over the ventricle minus the *l* belt), *i* (intermediate, corresponding to the region between *p* and MZ), and *m* (marginal, corresponding to the MZ), and plotted the percentages of pH3$^+$ cells falling in each of them (Figure 4B). We observed that the vast majority of pH3$^+$ cells were aligned along the ventricular surface, as proper apical progenitors, whereas only a few of them were scattered elsewhere. Up to P14, a few mitoses could be found in bin *p*, corresponding to the main zone where basal progenitors divide in placentals (Figure 4Ab, B). These mitoses were prevalently localized near the cortico-striatal notch, in the

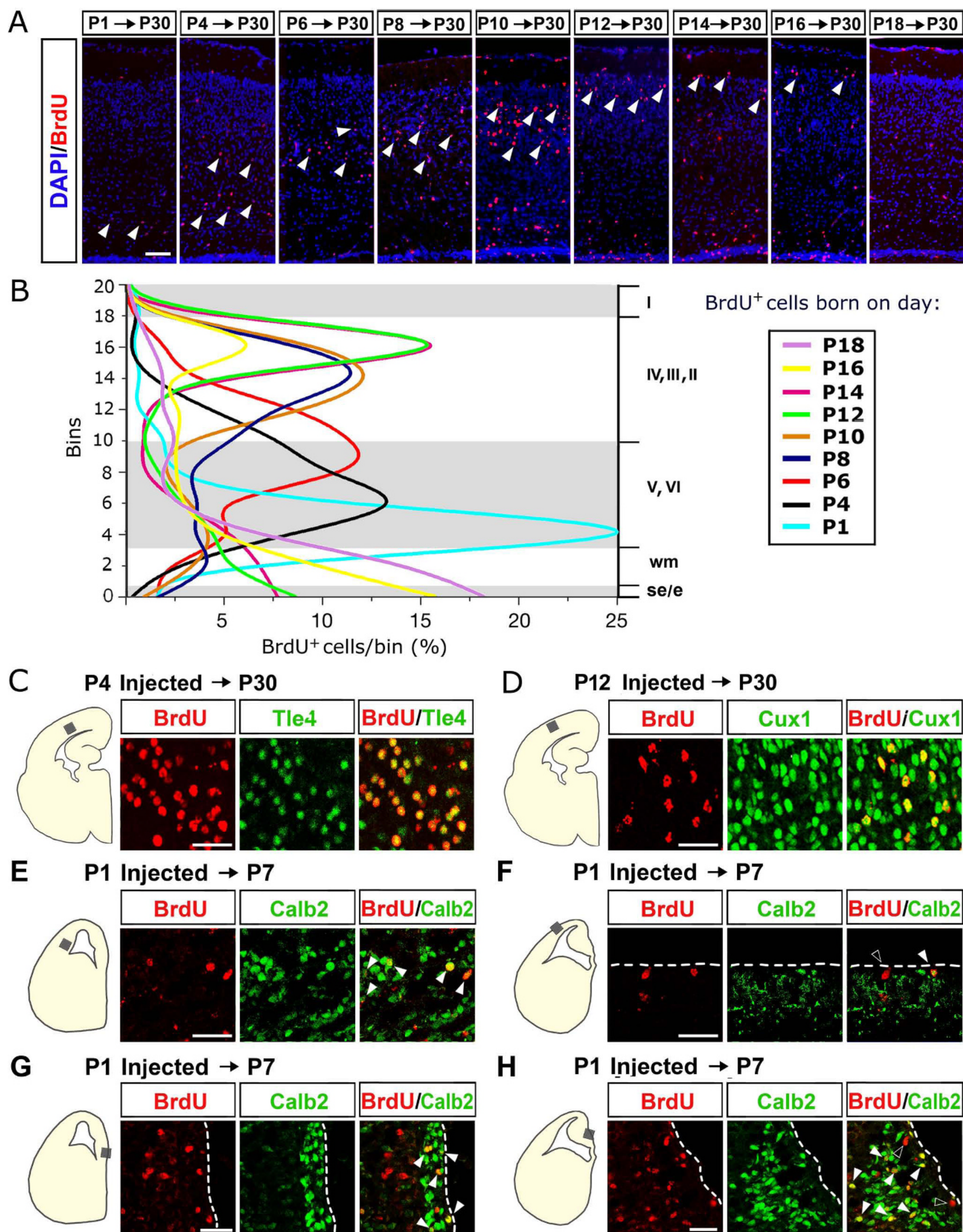

Figure 3 Bromodeoxyuridine birthdating of opossum neocortical neurons. **(A)** BrdU immunoprofiling of mid-frontal neocortical sections from opossums injected with a single pulse of BrdU at the ages of P1, P4, P6, P8, P10, P12, P14, P16 and P18, and fixed at P30. Arrowheads point to grey matter BrdU$^+$ cells. **(B)** Diagramatic representation of BrdU$^+$ cells sampled in (A): the cortical wall is divided into 20 equally spaced bins, numbered from ventricular to marginal; radial extension of cortical laminae is indicated by white/grey shading; plots representing percentages of BrdU$^+$ cells falling into each bin, for each injection time. **(C-H)** Colocalization of layer-specific markers, Tle4 (C), Cux1 (D), Calb2 (E-H), with BrdU injected at P4 (C), P12 (D) and P7 (E-H), respectively. Solid arrowheads in (E-H) point to Calb2$^+$/BrdU$^+$ cells; empty arrowheads in (F, H) point to Calb2$^-$/BrdU$^+$ cells. Abbreviations: I, II, III, IV, V, VI refer to cortical layers; e, ependyma; se, subependymal zone; wm, white matter. Scale bars: 100 μm in (A); 40 μm in (C-H).

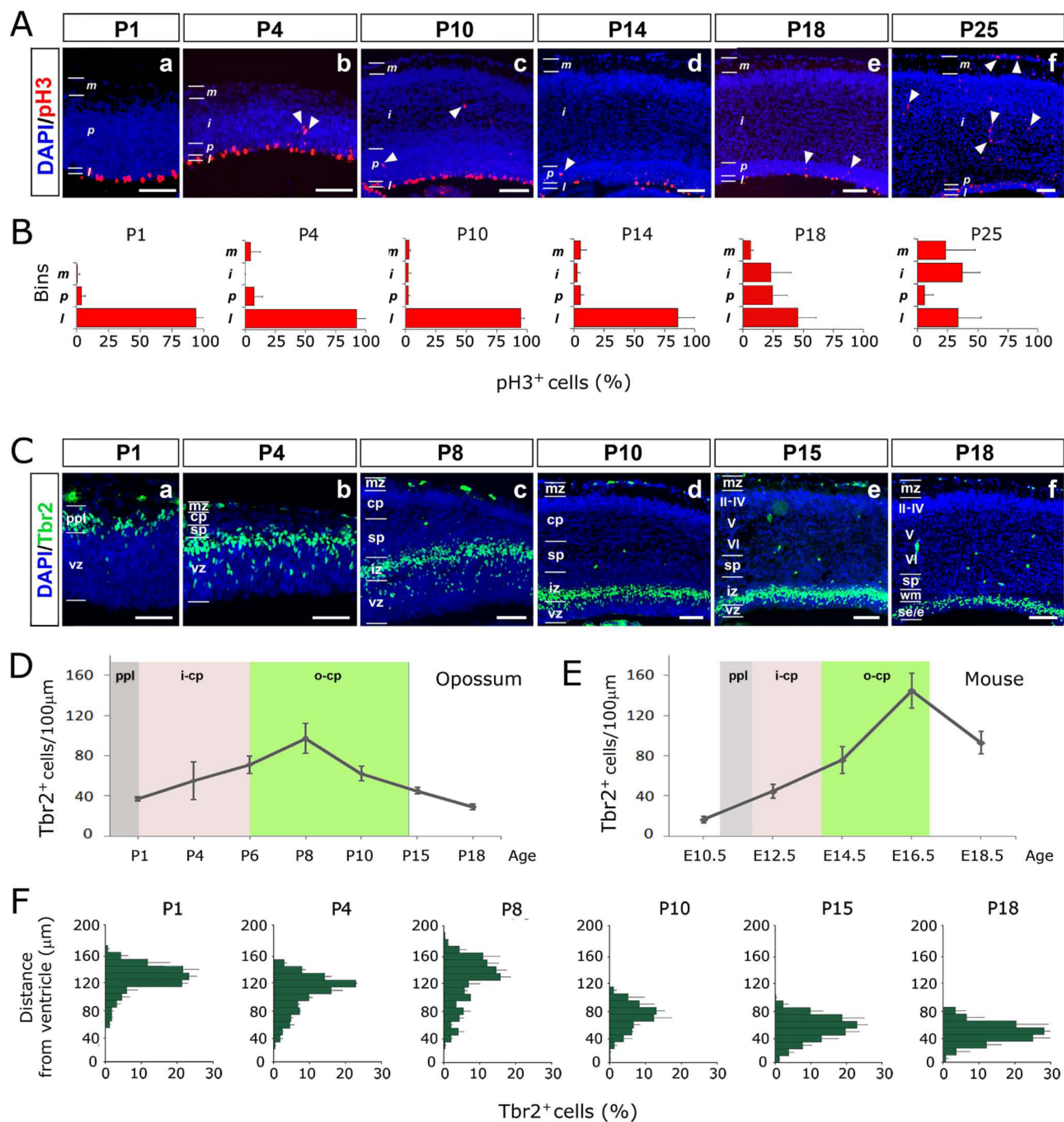

Figure 4 Dynamics of phospho-histone3 and Tbr2 expression in the developing opossum cortex. **(A)** Phospho-histone3 (pH3) immunoprofiling of mid-frontal neocortical sections of P1 to P25 opossums. Immunopositive cells are prevalently aligned near the ventricle; solid arrowheads point to rare abventricular pH3$^+$ mitotic cells. **(B)** Diagrammatic representation of pH3$^+$ cells sampled in (A). **(C)** Tbr2 immunoprofiling of mid-frontal neocortical sections of P1 to P18 opossums. **(D-F)**. Linear densities (D) and radial distributions (F) of Tbr2$^+$ cells sampled in (C). (E) Linear densities of Tbr2$^+$ cells in the mouse. Grey, pink and green shading in (D, E) demarcate peak neuronogenesis windows for primordial plexiform layer (ppl), inner cortical plate (i-cp) and outer cortical plate (o-cp), respectively. Abbreviations: II-IV, V, VI refer to cortical layers; cp, cortical plate; e, ependyma; iz, intermediate zone; mz, marginal zone; ppl, preplate; se, subependymal zone; sp, subplate; vz, ventricular zone; wm, white matter. Scale bars: 100 μm in (A, C).

presumptive paleocortical sector (Additional file 2). The frequency of *p* mitoses rose considerably after P18. Starting from this age, numerous abventricular mitoses could also be found in bins *i* and *m* (Figure 4Af, B), as described for placental MZ glial progenitors [32].

As a complementary approach, we looked for cortical expression of the T-box transcription factor Tbr2, a hallmark of basal progenitors in placentals [33]. We found numerous Tbr2$^+$ cells at all stages under examination, from P1 to P18 and later (Figure 4C and data not shown). On 10-μm-thick sections, their linear frequency gradually rose from 37 ± 2 cells/100 μm at P1 to 97 ± 14 cells/100 μm at P8 (P1 to P8 is the time window when PPL, deep CP and part of superficial CP are